A Journal of the Gesellschaft Deutscher Chemiker

Angewandte International Edition Chemie

GDCh

www.angewandte.org

Accepted Article

Title: Double-Caging Linker for AND-Type Fluorogenic Construction of Protein/Antibody Bioconjugates and in situ Quantification

Authors: Shiyong Liu, Guhuan Liu, Guohai Shi, Haoyue Sheng, Yanyan Jiang, and Haojun Liang

To be cited as: *Angew. Chem. Int. Ed.* 10.1002/anie.201702748
Angew. Chem. 10.1002/ange.201702748

Link to VoR: http://dx.doi.org/10.1002/anie.201702748
http://dx.doi.org/10.1002/ange.201702748

WILEY-VCH

10.1002/anie.201702748

WILEY-VCH

COMMUNICATION

Double-Caging Linker for AND-Type Fluorogenic Construction of Protein/Antibody Bioconjugates and *in situ* Quantification

Guhuan Liu,[a] Guohai Shi,[b] Haoyue Sheng,[b] Yanyan Jiang,[a] Haojun Liang,[a] and Shiyong Liu*[a]

Abstract: We report on *in situ* fluorescent quantification of the conjugation efficiency between azide-terminated synthetic polymers/imaging probes and thiol-functionalized antibodies/proteins/peptides, by utilizing a doubly caged profluorescent and heterodifunctional core molecule (**C1**) as the self-sorting bridging unit. Orthogonal dual 'click' coupling of **C1** with azide- and thiol-functionalized precursors leads to highly fluorescent bioconjugates, whereas single click products of **C1** remain essentially nonfluorescent. This 'AND' logic gate-type fluorogenic feature also enables further integration with FRET processes. For the construction of antibody-probe conjugates from an anti-carcinoembryonic antigen and a quinone-caged profluorescent naphthalimide derivative, the dual 'click' coupling process with **C1** can be conveniently monitored via emission turn-on of **C1**, whereas prominent changes in FRET ratios occur for antibody-imaging probe conjugates when specifically triggered by quinone oxidoreductase (NQO1), which is overexpressed in various types of cancer cells.

Covalent functionalization of proteins, peptides, and antibodies with synthetic polymers, drugs, and imaging probes affords clinically important protein-polymer conjugates[1] and antibody-drug conjugates.[2] The fabrication of these therapeutic bioconjugates relies on the appropriate choice of linker chemistries and high-efficiency 'click'-type conjugation reactions such as Staudinger ligation, Michael addition, copper-catalyzed azide-alkyne cycloaddition (CuAAC), and strain-promoted azide-cycloalkyne cycloaddition (SPAAC).[3] Further advancement in this field requires the introduction of new design criteria with features such as modular design, facile synthesis, and capability of being optically traced and multifunctional integration.

Traditionally, monitoring the formation of protein/antibody bioconjugates mainly relies on *ex situ* techniques such as sodium dodecyl sulfate-polyacrylamide gel electrophoresis (SDS-PAGE), mass spectrometry, high-performance liquid chromatography (HPLC), and gel permeation chromatography (SEC). This prohibits *in situ* real-time monitoring of bioconjugation processes. We envisage that endowing fluorescent monitoring and optically trackable features with protein/antibody bioconjugates would allow for the construction of theranostic bioconjugates with built-in diagnostic/imaging functions. The introduction of fluorogenic reactions into bioconjugates synthesis should enable the convenint monitoring of coupling efficiency and further integration with other photophysical processes. Previously, a variety of fluorogenic 'click' reactions between small molecule caged profluorophores and complementary reactive activators have been developed.[4] As fluorescence emission was only switched on when triggered by bioorthogonal reactions, background signals from excess probes were largely eliminated.

In the context of protein-polymer conjugates fabrication with fluorogenic coupling features, we are only aware of two relevant reports up to date.[5] In 2009, Cornelissen et al.[5a] reported fluorogenic CuAAC reaction between profluorescent 3-azido-coumarin-terminated PEG and alkyne-functionalized bovine serum albumin (BSA). O'Reilly and coworkers[5b] reported the fluorogenic conjugation of 2,3-dibromomaleimide-terminated PEG_{2k} onto salmon calcitonin (sCT). In both cases, the extent of bioconjugation could be *in situ* determined via emission changes resulting from '**single click**' fluorogenic reactions. However, as commonly practiced during 'grafting-to' fabrication of protein-polymer conjugates,[6] the chemical design is not modular as the reactive functionality need to be preinstalled on the PEG terminus.

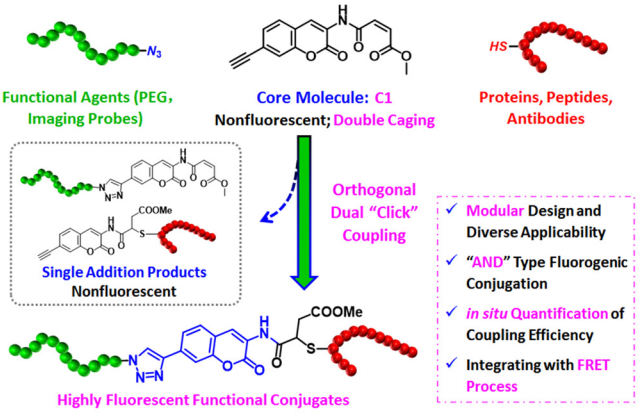

Scheme 1. Design strategy for *in situ* fluorescent quantification of the coupling efficiency between azide-terminated functional agents (e.g., molecular probes and PEG) and thiol-functionalized proteins/peptides/antibodies by utilizing doubly caged heterodifunctional **C1** as the self-sorting bridging unit. Orthogonal dual 'click' conjugation of **C1** with azide and thiol moieties leads to highly fluorescent functional bioconjugates, whereas single click products of **C1** remain essentially nonfluorescent.

We speculate that if heterodifunctional profluorophore containing **two orthogonal 'click' motifs** was utilized as the bridging linker, modular coupling of proteins/antibodies with polymers/imaging probes could be achieved if complementary reactive handles were installed. To introduce the fluorogenic feature for *in situ* assessment of the conjugation efficiency, the heterodifunctional profluorophore has to be **doubly caged** and only exhibits emission turn-on upon dual 'click'-enabled formation

[a] Dr. G. Liu, Dr. Y. Jiang, Prof. Dr. H. Liang, Prof. Dr. S. Liu
CAS Key Laboratory of Soft Matter Chemistry, Hefei National Laboratory for Physical Sciences at the Microscale, iChem (Collaborative Innovation Center of Chemistry for Energy Materials), Department of Polymer Science and Engineering
University of Science and Technology of China
96 Jinzhai Road, Hefei, Anhui Province 230026, China
E-mail: sliu@ustc.edu.cn
[b] Prof. Dr. G. Shi, H. Sheng
Department of Urology, Fudan University Shanghai Cancer Center, Department of Oncology, Shanghai Medical College
Fudan University
270 Dong'An Road, Shanghai 200032, China

Supporting information and the ORCID identification number(s) for the author(s) of this article can be found under http://dx.doi.org/10.1002/anie.201702748.

10.1002/anie.201702748

WILEY-VCH

COMMUNICATION

of conjugates. Herein, we report on the fluorogenic construction of protein-polymer and antibody-probe conjugates via orthogonal dual 'click' coupling with doubly caged profluorophore (Scheme 1). After preliminary structural screening and optimization, core molecule **C1** was chosen. This coumarin derivative contains heterodifunctional reactive moieties, which undergo CuAAC and Michael addition reactions with azide- and thiol-functionalized precursors, respectively. Serendipitously, 7-ethynyl and 3-alkenyl amide/ester functionalities of **C1** could serve as double fluorescence quenchers, and coumarin emission could only be switched-on upon 'AND'-type dual 'click' reactions. Since single 'click' reaction of **C1** with either thiol or azide-anchored precursors cannot lead to emission turn-on, **C1**-mediated coupling between azide-functionalized imaging probes/polymers and thiol-containing antibodies/proteins could be *in situ* optically monitored (Scheme 1).

The screening of doubly caged profluorescent core molecule with two distinct types of reactive moieties was a process of trial-and-error. At first, we came across with **C3** as a synthetic intermediate (Figure S1).[7] We observed that only dual CuAAC and Michael addition 'click' reactions of **C3** with azide- and thiol-containing molecules lead to a highly fluorescent product, whereas single click products of **C3** remain essentially nonfluorescent (Figure S1). Thus, **C3** obviously exhibits doubly caged fluorogenic behavior. However, we later found that the Michael addition reactivity of α,β-unsaturated ketone moiety in **C3** was quite low towards structurally hindered thiol moieties such as those in BSA proteins (Figure S1c).

We then designed heterodifunctional **C2** containing both propargyl ether and highly thiol-reactive alkenyl amide/ester moieties[8] as a possible candidate (Figure S2). Unfortunately, **C2** lacks double-caging fluorogenic behavior because Michael addition reaction of **C2** with mercaptoethanol (ME) already leads to emission turn-on (Figure S2b). In 2004, Fahrni and coworkers[4b] reported that 7-ethynyl-coumarin derivative could serve as a fluorogenic substrate and its click reaction with azide-containing molecules could switch on coumarin emission. This feature prompted us to design **C1** containing both 7-ethynyl and 3-alkenyl amide/ester moieties. Note that all screened core molecules (**C1**-**C3**) and synthetic intermediates were synthesized from commercially available starting materials (Scheme S1) and fully characterized (Figures S3-S6).

The orthogonal 'click' reactivity and fluorogenic feature of **C1** were then investigated (Figure 1a). Upon treating with both AP and ME, the emission intensity of **C1** at 415 nm increased ~77.8-fold within 2 h (Figures 1b). Meanwhile, coumarin emission exhibited no changes when **C1** was separately reacted with either AP or ME (Figure 1b). Thus, **C1** displays the desired double-caging fluorogenic feature. To further examine whether the emission enhancement of **C1** resulting from double 'click' reactions could be utilized for *in situ* quantifying the conjugation efficiency, single click products (**C1**-ME and AP-**C1**) were synthesized (Figures S7a-d), which are nonfluorescent (Figure 1c and S7f). For the CuAAC reaction between **C1**-Me and AP, HPLC analysis revealed the gradual formation of double 'click' product AP-**C1**-ME; meanwhile, **C1** emission intensities also increased and reached a maximum value (Figure 1c). On the other hand, thiol-ene reaction of AP-**C1** with ME was much faster (Figure S7f), indicating that CuAAC reaction is the rate-determining step during one-pot double 'click' reactions. Most importantly, emission intensities are linearly correlated with the coupling efficiency for both CuAAC and thiol-ene Michael addition fluorogenic reactions (Figure 1d and Figure S7f).

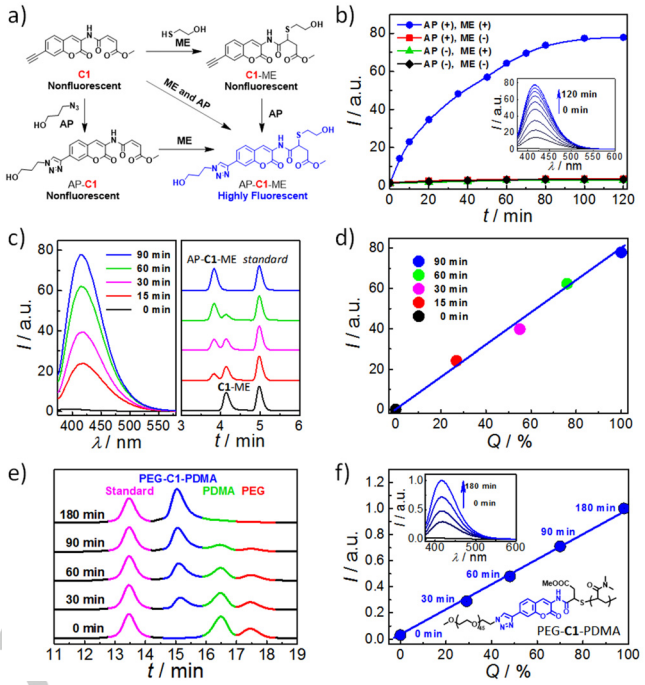

Figure 1. (a) Schematics for 'AND' logic-type fluorogenic reactions of doubly caged profluorescent **C1** with thiol- and azide-containing model compounds. (b) Emission intensities and fluorescence emission spectra (inset in b, λ_{ex} = 365 nm; with both ME and AP) recorded for **C1** (200 μM; PBS buffer containing 10 v/v% DMSO) upon reacting with or without ME (400 μM) in the presence or absence of AP (200 μM). Emission spectra (c, left), HPLC traces (c, right, methanol/H_2O 6/4 v/v; 254 nm absorbance), and correlation of emission intensities (λ_{em} = 420 nm) with conjugation efficiency (d) recorded for **C1**-ME upon reacting with AP in the presence of $CuSO_4$/Na-ascorbate. (e) DMF GPC traces (PEG_{20K} as external standard), (f) correlation of normalized emission intensities (~420 nm) with conjugation efficiency, and emission spectra (inset in f, λ_{ex} = 365 nm) recorded for *HS*-$PDMA_{37}$ (0.76 g/L) upon reacting with **C1** (200 μM) and PEG_{45}-N_3 (200 μM) in the presence of $CuSO_4$/Na-ascorbate.

The above results prompted us to further utilize doubly caged fluorogenic **C1** as a dually reactive core molecule for the modular fabrication of functional protein/antibody bioconjugates and *in situ* optically monitoring the conjugation process. As a model system, we then attempted to *in situ* quantify the 'click' coupling efficiency between azide- and thiol-functionalized polymer precursors by utilizing doubly caged **C1** as double-caging fluorogenic bridging linker. Thiol-terminated poly(dimethyl acrylamide) (*HS*-$PDMA_{37}$) (Figure S8) and azide end-functionalized PEG (PEG_{45}-N_3) were synthesized first. The coupling efficiency was quantified from traditional *ex situ* GPC results. **C1**-mediated double 'click' conjugation between PEG_{45}-N_3 and *HS*-PDMA required ~2-3 h to complete (Figure 1e), which was accompanied with a cumulative ~72-fold increase in emission intensity (Figure 1f inset). Intriguingly, linear correlation between the coupling efficiency and emission intensity was obtained (Figure 1f). Note that PEG_{45}-N_3, *HS*-$PDMA_{37}$, and **C1** linker were at 1:1:1 molar ratio, and the complete consumption of PEG_{45}-N_3 and *HS*-PDMA indicated that there was no need for further purification. To the best of our knowledge, this represents the first example of modular and fluorogenic construction of synthetic diblock copolymers,[9] and

10.1002/anie.201702748

the coupling efficiency could be monitored *in situ* using fluorescence technique (Scheme 1).

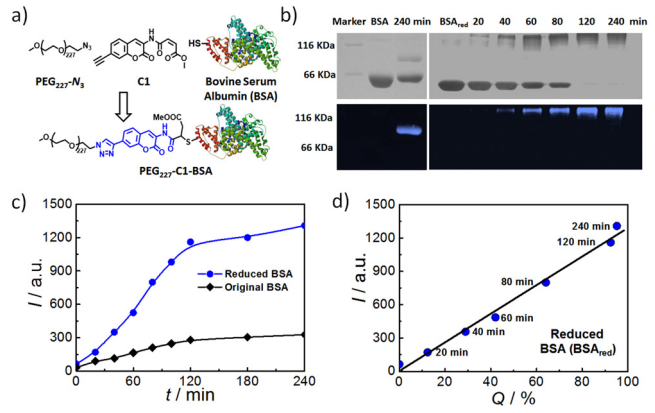

Figure 2. (a) Schematics for the conjugation of bovine serum albumin (BSA) or reduced BSA (BSA_{red}) with PEG_{227}-N_3 bridged by **C1**. (b) SDS-PAGE results recorded for 60 μM BSA (left) and reduced BSA (right) upon reacting with **C1** (600 μM) and PEG_{227}-N_3 (600 μM) in the presence of $CuSO_4$/Na-ascorbate. The upper row (with Coomassie blue staining) and lower row images in (b) were taken under white light and UV irradiation, respectively. (c) Time-dependent emission intensities (λ_{ex} = 365 nm, λ_{em} = 420 nm) recorded for original and reduced BSA (4 g/L, 60 μM) upon reacting with **C1** (600 μM) and PEG_{227}-N_3 (600 μM) in the presence of $CuSO_4$/Na-ascorbate. (d) Correlation of emission intensities (~420 nm) with protein conjugation efficiency determined via densitometric quantification of the SDS-PAGE data (b).

Next, we utilized **C1**-mediated double 'click' fluorogenic reactions to construct protein-polymer conjugates and quantify the conjugation efficiency. Thus, BSA was selected as a model protein, which contains a single free surface-exposed thiol moiety at Cys-34. The conjugation of PEG_{227}-N_3 with BSA by **C1** was then investigated (Figure 2a). Upon reacting with PEG-N_3 and native BSA in the presence of **C1**, the emission intensity gradually increased and tended to stabilize within ~4 h (Figure 2c). SDS-PAGE results revealed partial formation of fluorescent BSA-PEG conjugates and presence of considerable unreacted native BSA (Figure 2b, Figures S9a-S10). Densitometric quantification of gel electrophoresis bands revealed that >70% BSA remained intact after 4 h reaction time (Figure 2b). This should be due to the fact that the majority of Cys-34 residues in commercial BSA batches are in the oxidized form (~50% as quantified by Ellman's reagent).

We further investigated the fluorogenic conjugation between PEG_{227}-N_3 and reduced BSA, in which the reduction of disulfide linkages by tris(2-carboxyethyl)phosphine hydrochloride (TCEP) liberates more free thiol moieties. Significantly higher emission intensities were observed within ~4 h (Figure 2c). Complete consumption of reduced BSA and formation of BSA-PEG conjugates could be achieved within ~3-4 h (Figure 2b and Figure S9c). Not that only the gel electrophoresis bands of PEG-***C1***-BSA conjugates emit fluorescence (Figure 2b). Most importantly, a linear correlation between the conjugation efficiency and emission intensities was obtained (Figure 2d).

Antibody-directed molecular imaging offers huge potentials for medical diagnosis and evaluation of therapeutic responses, and could be directly integrated with surgical or endoscopic procedures.[2] As a further demonstration, we constructed functional antibody-imaging probe bioconjugates via **C1**-mediated modular approach (Scheme 1 and Figure 3). Fluorescence emission of the conjugated probe, QNAM (Figure S11), was initially caged by covalently linked trimethyl-locked quinone (Q3PA), but could be selectively switched on via quinone oxidoreductase (NQO1)-triggered cleavage.[10] Thus, for the antibody-imaging probe ensemble, FRET between bridging coumarin chromophore and naphthalimide (NAM) will occur. NQO1, overexpressed up to ~50-fold in the cytosolic milieu of various human tumor cells could then be detected and quantified in a ratiometric fluorescent manner. ACEA, anti-carcinoembryonic antigen, was chosen to construct antibody-probe conjugates, as CEA is also overexpressed in most types of carcinomas (Scheme 1 and Figure 3a).

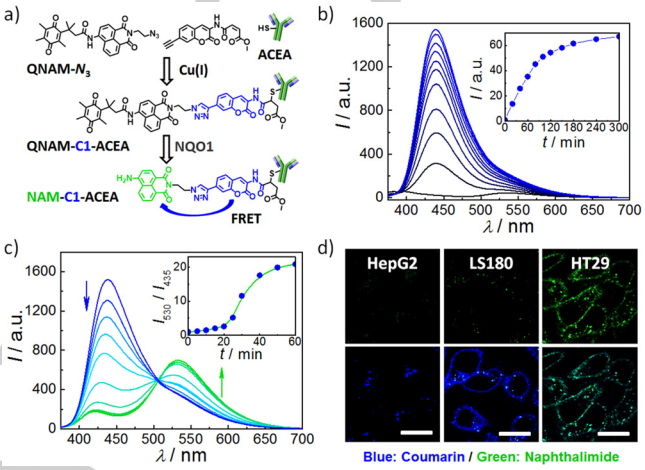

Figure 3. (a) Schematics for the fabrication of antibody-imaging probe conjugates from ACEA and fluorescently caged naphthalimide (QNAM-N_3) via double click reactions with **C1**, and subsequent enzyme-triggered turn-on of FRET process. Emission spectra (b, λ_{ex} = 365 nm) and emission intensities (inset in b, λ_{em} = 435 nm) recorded for QNAM-N_3 (2.5 mM) upon reacting with **C1** (2.5 mM) and ACEA (1 mg/mL) in the presence of $CuSO_4$/Na-ascorbate. (c) Emission spectra (λ_{ex} = 365 nm) and (inset in c) time-dependent emission intensity ratios, I_{530nm}/I_{435nm}, recorded for QNAM-**C1**-ACEA (1 mg/L) upon treating with NQO1 enzyme (20 ng/mL) and NADPH (10 μM). (d) Representative blue channel (coumarin, 430±20 nm) and green channel (naphthalimide, 530±20 nm) CLSM images (scar bar: 10 μm) recorded for HepG2 (CEA-deficient, NQO1-deficient), LS180 (CEA-positive, NOQ1-deficient), and HT29 (CEA-positive, NQO1-positive) cells upon incubating with QNAM-**C1**-ACEA (0.05 mg/mL) for 12 h; the bottom row represents an overlay of blue and green channel images.

During **C1**-mediated 'AND'-type fluorogenic conjugation of ACEA with QNAM-N_3, we could only observe the gradual enhancement of emission band at ~435 nm, corresponding to the emission turn-on of **C1** linker (Figure 3b). Note that NAM emission at ~530 nm was still caged by Q3PA. A cumulative ~66-fold increase in emission intensity was recorded during conjugation. Thus, we could *in situ* quantify the conjugation efficiency based on emission intensity changes of **C1**.

Upon co-incubating with NADPH/NQO1, emission intensity of QNAM-N_3 precursor at ~540 nm increased ~52 times (Figures S12). Moreover, the emission band of AP-**C1**-ME overlaps with the excitation band of NQO1-treated QNAM-N_3, but not with that of original QNAM-N_3 (Figure S13). During co-incubating of QNAM-**C1**-ACEA bioconjugates with NADPH/NQO1, a prominent increase of NAM emission intensities (~530 nm) was observed, which was accompanied with a considerable reduction in **C1** emission at ~435 nm. Within ~1 h, ~20-fold change in FRET ratios (I_{530nm}/I_{435nm}) was recorded (Figure 3c inset). The above results

10.1002/anie.201702748

indicated effective FRET between **C1** linker and enzymatically generated NAM residues. The abrupt changes in FRET intensity ratios suggested that the antibody-probe conjugates could serve as an excellent probe for the assay of NQO1 enzyme levels and bioactivities. Compared to previous works by McCarley and coworkers[10] concerning single emission band-based NQO1 molecular probes, fluorogenically fabricated QNAM-**C1**-ACEA hybrid probes provide advantages including self-calibration, ratiometric fluorescent detection, and enhanced selectivity and site-specificity.

Advantageous features described above for QNAM-**C1**-ACEA hybrid probes prompted us to further explore the possibility of differentiating among different types of cancer cells based on CEA level and NQO1 level/bioactivity. We exposed live HepG2 (CEA-deficient, NQO1-deficient), LS180 (CEA-positive, NOQ1-deficient), and HT29 (CEA-positive, NQO1-positive) cells to QNAM-**C1**-ACEA bioconjugates. Confocal laser scanning microscopy (CLSM) images of LS180 cells revealed the presence of punctuated blue-emitting dots of **C1** linker and minimal NAM green emission signals inside the cells (Figure 3d), indicating significant cellular uptake of QNAM-**C1**-ACEA and its intracellular stability due to the lack of cytosolic NQO1. For CEA-positive and NQO1-positive colon cancer cells (HT29), the green channel NAM emission was considerably enhanced and almost co-localized with blue channel emission of **C1** linker. Note that intensity of the latter was reduced to some extent due to the occurrence of FRET process (Figure 3c). On the other hand, CEA-deficient and NQO1-deficient HepG2 cells treated with QNAM-**C1**-ACEA revealed extremely low blue and low green emissions (Figure 3d). Since NQO1 enzyme is mainly located within the cytosolic milieu of certain types of cancer cells, the above results indicated that QNAM-**C1**-ACEA probe could only display strong green NAM emission in an 'AND' logic gate-type manner (i.e., both CEA-positive and NQO1-positive cellular milieu is required). Intriguingly, this is quite comparable to the **C1**-mediated 'AND'-type fluorogenic fabrication process for QNAM-**C1**-ACEA bioconjugates from ACEA and QNAM-N_3 precursor (Scheme 1 and Figures 3a-3b).

In summary, we reported the screening of doubly caged heterodifunctional and profluorescent **C1** possessing orthogonal dual 'click' motifs. **C1**-mediated 'AND'-type fluorogenic and modular construction of functional conjugates allows for facile *in situ* quantification of the coupling efficiency via single band emission intensity changes. Fluorogenically constructed antibody-imaging probe conjugates, QNAM-**C1**-ACEA, could selectively detect oxidoreductase such as NQO1 in a ratiometric fluorescent manner. The reported double-caging strategy and associated modular/fluorogenic fabrication of functional protein/antibody conjugates could further be generalized to integrate with other types of bioorthogonal chemistries.

Acknowledgements

The financial support from National Natural Science Foundation of China (NNSFC) Project (51690150, 51690154, 21674103, and 21504087) and International S&T Cooperation Program of China (ISTCP) of MOST (2016YFE0129700) is gratefully acknowledged.

Keywords: bioconjugates • prodrugs • click chemistry • FRET • fluorescent probes

[1] a) R. Duncan, *Nat. Rev. Drug Discovery* **2003**, *2*, 347-360; b) H. A. Klok, *Macromolecules* **2009**, *42*, 7990-8000; c) E. M. Pelegri-O'Day, E.-W. Lin, H. D. Maynard, *J. Am. Chem. Soc.* **2014**, *136*, 14323-14332; d) I. Cobo, M. Li, B. S. Sumerlin, S. Perrier, *Nat. Mater.* **2015**, *14*, 143-159.

[2] a) L. Ducry, B. Stump, *Bioconjugate Chem.* **2010**, *21*, 5-13; b) P. Agarwal, C. R. Bertozzi, *Bioconjugate Chem.* **2015**, *26*, 176-92; c) N. Krall, F. P. da Cruz, O. Boutureira, G. J. L. Bernardes, *Nat. Chem.* **2016**, *8*, 103-113.

[3] a) M. P. Deonarain, G. Yahioglu, I. Stamati, J. Marklew, *Expert Opin. Drug Discov.* **2015**, *10*, 463-81; b) V. Chudasama, A. Maruani, S. Caddick, *Nat. Chem.* **2016**, *8*, 114-119; c) L. A. Canalle, D. W. P. M. Lowik, J. C. M. van Hest, *Chem. Soc. Rev.* **2010**, *39*, 329-353.

[4] a) J. E. T. Corrie, *J. Chem. Soc.-Perkin Trans. 1* **1994**, 2975-2982; b) Z. Zhou, C. J. Fahrni, *J. Am. Chem. Soc.* **2004**, *126*, 8862-8863; c) K. Sivakumar, F. Xie, B. M. Cash, S. Long, H. N. Barnhill, Q. Wang, *Org. Lett.* **2004**, *6*, 4603-4606; d) C. Le Droumaguet, C. Wang, Q. Wang, *Chem. Soc. Rev.* **2010**, *39*, 1233-1239; e) P. Shieh, C. R. Bertozzi, *Org. Biomol. Chem.* **2014**, *12*, 9307-9320.

[5] a) A. J. Dirks, J. J. L. M. Cornelissen, R. J. M. Nolte, *Bioconjugate Chem.* **2009**, *20*, 1129-1138; b) M. P. Robin, P. Wilson, A. B. Mabire, J. K. Kiviaho, J. E. Raymond, D. M. Haddleton, R. K. O'Reilly, *J. Am. Chem. Soc.* **2013**, *135*, 2875-2878.

[6] a) J. Geng, G. Mantovani, L. Tao, J. Nicolas, G. Chen, R. Wallis, D. A. Mitchell, B. R. G. Johnson, S. D. Evans, D. M. Haddleton, *J. Am. Chem. Soc.* **2007**, *129*, 15156-15163; b) T. H. Nguyen, S.-H. Kim, C. G. Decker, D. Y. Wong, J. A. Loo, H. D. Maynard, *Nat. Chem.* **2013**, *5*, 221-227; c) D. Moatsou, J. Li, A. Ranji, A. Pitto-Barry, I. Ntai, M. C. Jewett, R. K. O'Reilly, *Bioconjugate Chem.* **2015**, *26*, 1890-1899; d) D. Bacinello, E. Garanger, D. Taton, K. C. Tam, S. Lecommandoux, *Biomacromolecules* **2014**, *15*, 1882-1888; e) C. K. Wong, A. J. Laos, A. H. Soeriyadi, J. Wiedenmann, P. M. G. Curmi, J. J. Gooding, C. P. Marquis, M. H. Stenzel, P. Thordarson, *Angew. Chem. Int. Ed.* **2015**, *54*, 5317-5322; *Angew. Chem.* **2015**, *127*, 5407-5412.

[7] Y. Jiang, G. Liu, X. Wang, J. Hu, G. Zhang, S. Liu, *Macromolecules* **2015**, *48*, 764-774.

[8] L. Yi, H. Li, L. Sun, L. Liu, C. Zhang, Z. Xi, *Angew. Chem. Int. Ed.* **2009**, *48*, 4034-4037; *Angew. Chem.* **2009**, *121*, 4094-4097.

[9] a) P. L. Golas, K. Matyjaszewski, *Chem. Soc. Rev.* **2010**, *39*, 1338-1354; b) P. Espeel, F. E. Du Prez, *Macromolecules* **2015**, *48*, 2-14; c) J. M. Hu, S. Y. Liu, *Macromolecules* **2010**, *43*, 8315-8330.

[10] a) S. U. Hettiarachchi, B. Prasai, R. L. McCarley, *J. Am. Chem. Soc.* **2014**, *136*, 7575-7578; b) Q. A. Best, A. E. Johnson, B. Prasai, A. Rouillere, R. L. McCarley, *ACS Chem. Biol.* **2016**, *11*, 231-240; c) W. C. Silvers, B. Prasai, D. H. Burk, M. L. Brown, R. L. McCarley, *J. Am. Chem. Soc.* **2013**, *135*, 309-314.

10.1002/anie.201702748

WILEY-VCH

Entry for the Table of Contents

COMMUNICATION

Fluorogenic Bioconjugates: Doubly caged profluorescent and heterodifunctional core molecules were screened, and used for orthogonal dual 'click' reactions to fabricate functional protein/antibody bioconjugates. Both conjugate formation and subsequent imaging probe activation could be *in situ* quantified via fluorescence emission intensity and FRET ratio changes, respectively.

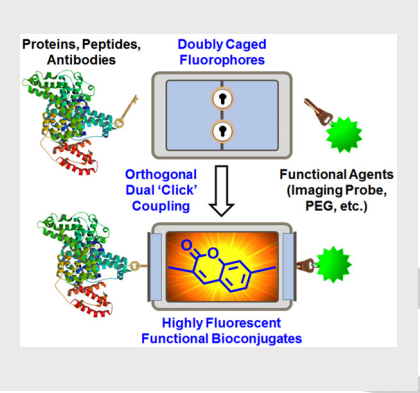

*G. Liu, G. Shi, H. Sheng, Y. Jiang, H. Liang, S. Liu**

Page No. – Page No.

Double-Caging Linker for AND-Type Fluorogenic Construction of Protein/ Antibody Bioconjugates and *in situ* Quantification